

# Long-range transfer of electron-phonon coupling in oxide superlattices

N. Driza, S. Blanco-Canosa, M. Bakr, S. Soltan, M. Khalid, L. Mustafa, K. Kawashima, G. Christiani, H.-U. Habermeier, G. Khaliullin, C. Ulrich, M. Le Tacon, and B. Keimer

The targeted manipulation of the electronic properties of metal-oxide heterostructures and superlattices with atomically precise interfaces is currently at the frontier of materials research. Control parameters including the layer thickness and composition as well as epitaxial strain and gate fields have allowed systematic tuning of many-body phenomena such as ferroelectricity, magnetic order, and superconductivity. The impact of static interfacial lattice distortions on some of these phenomena has already been recognized, but the influence of the dynamical electron-phonon interaction on the electronic properties of artificially layered structures has thus far not been addressed, despite evidence for its crucial role for the phase behavior of bulk transition metal oxides. The electron-phonon interaction is of central importance for the electrical and thermal properties of solids, and its influence on superconductivity, colossal magnetoresistance, and other many-body phenomena in correlated-electron materials is currently the subject of intense research. However, the non-local nature of the interactions between valence electrons and lattice ions, often compounded by a plethora of vibrational modes, present formidable challenges for attempts to experimentally control and theoretically describe the physical properties of complex materials.

Here we report a Raman scattering study of the lattice dynamics in superlattices (SLs) of the high-temperature superconductor  $\text{YBa}_2\text{Cu}_3\text{O}_7$  (YBCO) and the colossal-magnetoresistance compound  $\text{La}_{2/3}\text{Ca}_{1/3}\text{MnO}_3$  (LCMO) that suggests a new approach to this problem. [1] Our study brings together two previously disconnected areas of research. On the one hand, YBCO-LCMO SLs have served as model systems for the interplay between the antagonistic order parameters of the constituent materials, and for interfacial spin and orbital reconstructions. [2] On the other hand, prior research has shown that the electron-phonon interaction and its interplay with electronic correlations determines the competition between superconducting and other forms of electronic order in bulk YBCO, and between correlated metallic and polaronic insulating states in bulk LCMO. In bulk compounds, pressure and chemical substitution offer only limited options to tune this interplay. The outcome of our study identifies the superlattice geometry as a powerful new tool to systematically modify the electron-phonon interaction in complex materials.

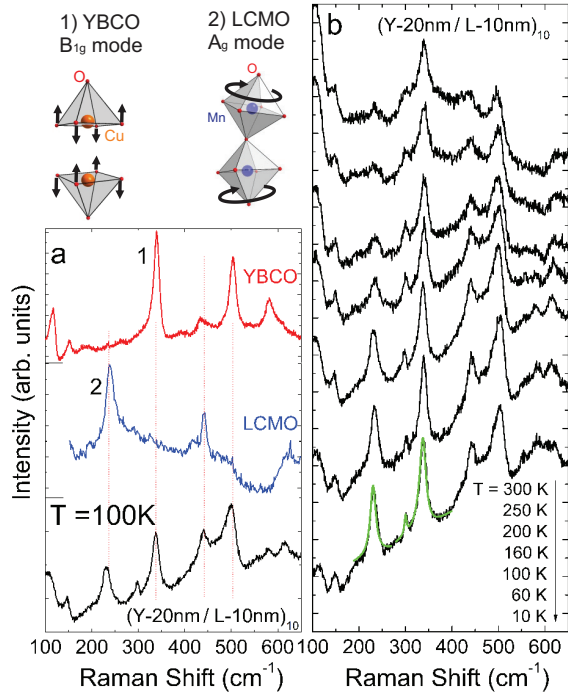


Figure 1: (a) Raman spectra of pure YBCO, LCMO, and a  $(\text{Y-20 nm/L-10 nm})_{10}$  superlattice at  $T = 100\text{ K}$ . 1 and 2 denote the peaks corresponding to the  $B_{1g}$   $340\text{ cm}^{-1}$  out-of-phase  $c$ -axis polarized vibration of the planar oxygen atoms in YBCO, and the  $230\text{ cm}^{-1}$   $A_g$  in-phase rotation of the  $\text{MnO}_6$  octahedra of LCMO, respectively. The sketches provide pictorial representations of the vibration patterns. (b) Temperature dependence of the Raman spectra of a  $(\text{Y-20 nm/L-10 nm})_{10}$  superlattice in  $xx$  polarization. For clarity each spectrum is vertically shifted by a constant offset.

Our experiments were performed on SLs with 10 nm thick LCMO layers, and YBCO layers ranging in thickness

from 10 to 50 nm, grown epitaxially on SrTiO<sub>3</sub> by pulsed laser deposition. Figure 1(a) shows a typical Raman spectrum measured on a SL comprising 10 repetitions of 20 nm thick YBCO and 10 nm thick LCMO layers (hereafter referred to as (Y-20 nm/L-10 nm)<sub>10</sub>), along with reference spectra of 300 nm thick YBCO and LCMO films. Both reference and SL spectra exhibit two prominent low-energy modes at 230 and 340 cm<sup>-1</sup>, which arise from antiphase rotations of the MnO<sub>6</sub> octahedra in LCMO and vibrations of the in-plane oxygen atoms perpendicular to the CuO<sub>2</sub> layers in YBCO, respectively (see Fig. 1 for the vibration patterns).

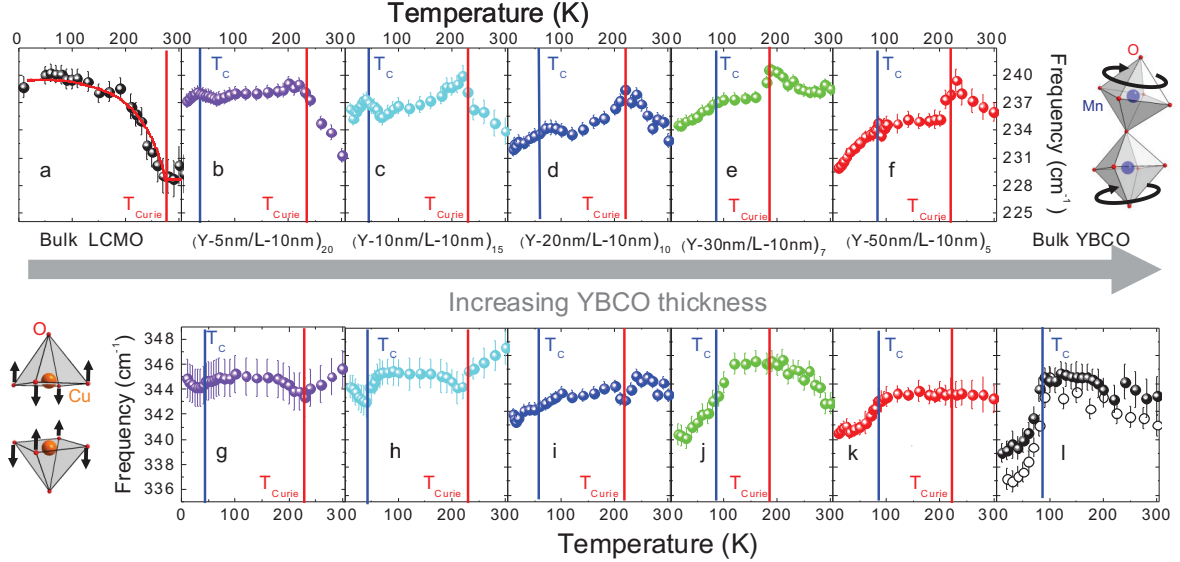


Figure 2: Temperature dependence of the  $A_g$  LCMO phonon frequency (a-f), and of the  $B_{1g}$  YBCO phonon frequency (g-l) of the different samples studied here. Panel (j) shows the temperature dependence of the  $B_{1g}$  mode frequency measured on a 300 nm thick film (black spheres) and single crystal (open circles).

The two low-energy vibrations have been the focus of extensive prior investigations on bulk samples, which have established that they are subject to strong electron-phonon interactions. The influence of the electron-phonon interaction can be recognized in the lineshapes of the Raman profiles and in their temperature dependence. The interaction of a discrete phonon mode with a continuum of electronic excitations leads to an asymmetric lineshape. Moreover, phonon modes with strong electron-phonon coupling tend to exhibit lineshape anomalies at electronically driven phase transitions, as a consequence of modifications of the electronic charge or spin excitation spectra. In particular, the mode with  $B_{1g}$  symmetry at 340 cm<sup>-1</sup> in bulk YBCO (marked “1” in Fig. 1) shows pronounced superconductivity-induced lineshape anomalies that are due to the loss of electron-phonon decay channels below the superconducting energy gap.

We first discuss the data on the  $B_{1g}$  phonon in YBCO, which are highlighted in Fig. 2. The phonon energy softens below the superconducting  $T_c$ , as a result of the loss of electron-phonon decay channels for phonon energies below the superconducting energy gap. The amplitude of the softening decreases progressively with decreasing YBCO layer thickness in the YBCO-LCMO superlattices (Fig. 2(c)). This indicates a loss of mobile charge carriers in the CuO<sub>2</sub> planes with decreasing YBCO layer thickness in the SLs, which is at least in part a consequence of the charge transfer across the YBCO-LCMO interface known from prior work. [2] The LCMO mode with  $A_g$  symmetry at 230 cm<sup>-1</sup> in LCMO (marked “2” in Fig. 1) shows anomalous behavior at the high-temperature ferromagnetic transition which is discussed in detail elsewhere. [1]

Here we highlight the surprising behavior of the LCMO  $A_g$  mode at low temperatures. Although the mode energy (and hence presumably the vibration pattern) are close to the ones observed in bulk LCMO, the mode exhibits a strong anomaly at the *superconducting* transition temperature  $T_c$  of YBCO (Fig. 2). The amplitude of the superconductivity-induced softening ( $\sim 2\%$  of the mode energy in the (Y-50 nm/L-10 nm)<sub>5</sub> sample) is comparable to the one of the YBCO  $B_{1g}$  oxygen vibration, which exhibits by far the strongest superconductivity-induced anomaly of any of the Raman-active phonons in bulk YBCO. Figure 3 shows that the frequency shift of the LCMO  $A_g$  mode goes along with an equally pronounced narrowing of the linewidth, again analogous to the one observed for the YBCO  $B_{1g}$  mode. This implies that the electron-phonon coupling in the YBCO layers is transferred to a vibrational mode in the LCMO layers of the SL. The superconductivity-induced redshift of

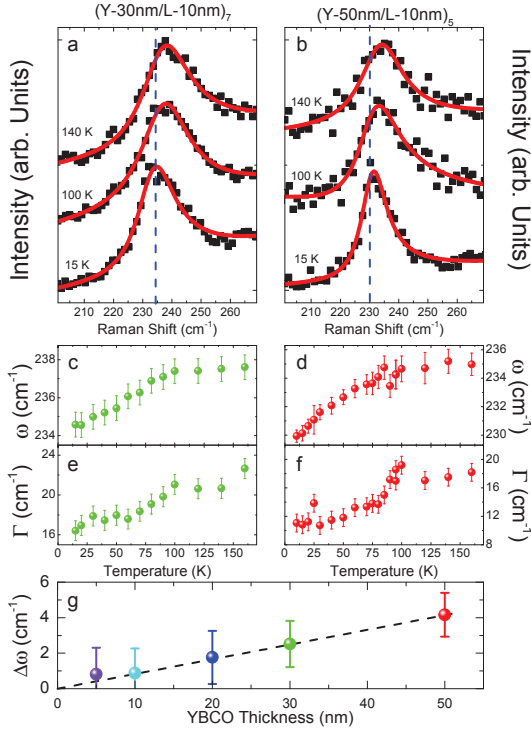


Figure 3: (a) LCMO  $A_g$  phonon at  $T = 140, 100$  and  $15$  K in a  $(Y-30 \text{ nm}/L-10 \text{ nm})_7$  superlattice. The black squares are the experimental data points, and the red lines are the results of fits to Fano profiles. (b) LCMO  $A_g$  phonon at  $140, 100$  and  $15$  K in a  $(Y-50 \text{ nm}/L-10 \text{ nm})_7$  superlattice. (c) Temperature dependence of the frequency of the LCMO  $A_g$  mode in a  $(Y-30 \text{ nm}/L-10 \text{ nm})_7$  superlattice. (d) Temperature dependence of the frequency of the LCMO  $A_g$  mode in a  $(Y-50 \text{ nm}/L-10 \text{ nm})_7$  superlattice. (e) Temperature dependence of the linewidth of the LCMO  $A_g$  mode in a  $(Y-30 \text{ nm}/L-10 \text{ nm})_7$  superlattice. (f) Temperature dependence of the linewidth of the LCMO  $A_g$  mode in a  $(Y-50 \text{ nm}/L-10 \text{ nm})_7$  superlattice. (g) YBCO thickness dependence of the  $A_g$  LCMO phonon softening through  $T_c$  in our superlattices.

the LCMO  $A_g$  mode scales linearly with the thickness of the YBCO layers over a remarkably long range of at least  $50 \text{ nm}$  (Fig. 3(g)). This observation indicates that long-range Coulomb interactions, whose influence on the static lattice structure of heterostructures and superlattices composed of covalently bonded transition metal oxides has already been recognized, play a key role in the lattice dynamics and electron-phonon interaction in such structures as well.

A possible explanation of the anomalous behavior of the LCMO  $A_g$  mode in our YBCO-LCMO SLs is a small copper-oxygen admixture to the vibration pattern induced by the strong Cu-O-Mn bond [2] across the YBCO-LCMO interface, in combination with long-range, poorly screened Coulomb interactions which ensure that the entire YBCO layer participates in the combined mode. The superconductivity-induced anomaly suggests that the copper-oxygen component dominates the self-energy of the hybrid mode, despite its small amplitude. This scenario requires one or several YBCO phonons that hybridize efficiently with the LCMO  $A_g$  mode and experience a large electron-phonon coupling. An interesting candidate is the odd-parity ( $B_{1u}$ ) counterpart of the  $340 \text{ cm}^{-1}$  ( $B_{1g}$ ) mode, which is “silent” (i.e. unobservable by Raman and infrared spectroscopies) in pure YBCO. According to density-functional calculations, [3] this mode is nearly degenerate with LCMO  $A_g$  phonon. The calculations also predict a strong electron-phonon coupling parameter for this mode, which is actually the most attractive in the d-wave Cooper pairing channel among all phonons in YBCO. If the space-group symmetry of the superlattice allows any mixing with the LCMO  $A_g$  mode, the two nearly degenerate modes will hybridize. The effect of superconductivity on the hybrid mode will then mirror the one of the  $B_{1u}$  mode, which is invisible in bulk YBCO because of its “silent” character. This effect is expected to be substantial because of the large electron-phonon coupling of the  $B_{1u}$  vibration.

While detailed calculations are required to substantiate this scenario and to further elucidate the origin of the observed long-range transfer of electron-phonon coupling, the data at hand already demonstrate that epitaxial superlattices offer novel opportunities to generate vibrational modes that do not exist in the bulk, and to systematically modify their properties through the layer geometry. This provides a powerful new tool to explore and control the electron-phonon interaction in transition metal oxides at ambient pressure and without introducing chemical disorder.

#### References:

- [1] Driza, N. *et al.* Nature Materials **11**, 675–681 (2012).
- [2] Chakhalian, J. *et al.* Science **318**, 1114–1117 (2007).
- [3] Heid R., R. Zeyher, D. Manske, K.-P. Bohnen. Physical Review B **80**, 024507 (2009).